Obrabotka metallov (tekhnologiya, oborudovanie, instrumenty) = Metal Working and Material Science. 2025 vol. 27 no. 3 pp. 151–165
ISSN: 1994-6309 (print) / 2541-819X (online)
DOI: 10.17212/1994-6309-2025-27.3-151-165

NSTU NETI

Obrabotka metallov - Metal Working and Material Science

Journal homepage: http://journals.nstu.ru/obrabotka_metallov

Corrosion properties of coatings produced from self-fluxing powders by the detonation spraying method

Vyacheslav Sirota [a, *], ***Dmitrii Prokhorenkov*** [b], ***Anton Churikov*** [c], ***Daniil Podgorny*** [d], ***Natalia Alfimova*** [e], ***Andrey Konnov*** [f]

Belgorod State Technological University named after V.G. Shukhov, 46 Kostyukova st., Belgorod, 308012, Russian Federation

[a] https://orcid.org/0000-0003-4634-7109, zmas36@mail.ru; [b] https://orcid.org/0000-0002-6455-8172, bstu-cvt-sem@yandex.ru;
[c] https://orcid.org/0000-0002-1829-2676, churikov.toni@mail.ru; [d] https://orcid.org/0000-0001-7435-5005, dan_podgor@mail.ru;
[e] https://orcid.org/0000-0003-3013-0829, alfimovan@mail.ru; [f] https://orcid.org/0009-0009-3245-0747, andrekonnov555@yandex.ru

ARTICLE INFO

Article history:
Received: 07 May 2025
Revised: 06 June 2025
Accepted: 24 June 2025
Available online: 15 September 2025

Keywords:
Detonation spraying
Corrosion properties of coatings

Funding
The research was conducted as part of Comprehensive Project No. 30/22 dated October 12, 2022, under Agreement No. 075-11-2025-026 of February 27, 2025: "Development of High-Tech Production of Composite Cutting Elements for Machinery and Thermal Equipment in Agricultural Product Processing".

Acknowledgements
The study was performed using equipment from the High Technologies Center of BSTU named after V.G. Shukhov.

ABSTRACT

Introduction. This paper presents the results of a comprehensive study of the corrosion properties of innovative coatings based on self-fluxing *NiCrBSi* alloys (*PR-NKh17SR4*) modified with 10 wt.% boron carbide (B_4C) nanoparticles, produced by detonation spraying. The relevance of the study stems from the critical need to develop new high-performance materials for protecting essential equipment operating under extreme conditions, including marine environments, chemically aggressive solutions, and elevated temperatures. Particular attention is paid to a detailed analysis of the influence of B_4C on corrosion mechanisms, the formation of protective passivating layers, and the relationship between microstructure and functional properties of the coatings. **Objective.** A comprehensive evaluation of the effect of 10 wt.% B_4C addition on the corrosion resistance, microstructure, and mechanical properties of coatings in comparison with the base alloy *NiCrBSi* alloy (*PR-NKh17SR4*) and the commercially available counterpart *NiCr/WC* alloy (*VSNGN-85*), widely used in industry. **Methods.** The coatings were applied to *0.40% C-Mn* steel substrates using a multi-chamber cumulative detonation spraying unit (*MKDU*). Modern analytical methods were employed for thorough characterization: scanning electron microscopy (*SEM*, *Mira 3*) with energy-dispersive spectroscopy, X-ray diffraction (*XRD*, *ARL X'TRA* diffractometer) with quantitative phase composition assessment using the *Rietveld* method. Corrosion tests were conducted in a 3.5% *NaCl* solution simulating marine environments, using potentiostatic measurements and electrochemical impedance spectroscopy on a *SmartStat PS-10-4* potentiostat-galvanostat. The depth of corrosion penetration was evaluated using confocal laser microscopy (*Lext OLS5000*) with a resolution of 10 nm. **Results and discussion.** It was established that the addition of 10 wt.% B_4C leads to the formation of a unique multilayered coating structure with an amorphous phase content of up to 12.3% and promotes the formation of passivating chromium (Cr_2O_3) and boron (B_2O_3) oxides. Electrochemical measurements revealed an exceptionally low corrosion rate of 0.0014 mm/year, which is an order of magnitude lower than that of the base alloy (0.021 mm/year) and 30 times lower than that of the commercial counterpart *NiCr/WC* alloy (*VSNGN-85*) (0.041 mm/year). The modified coating exhibits remarkably high polarization resistance (215±25 kΩ·cm²) and minimal porosity (0.6±0.1%). The microhardness reached 680±40 HV, significantly exceeding that of the base alloy (520±30 HV), which is attributed to the formation of dispersed NiB_2 particles. *XRD* and *EDS* analyses confirmed the catalytic effect of B_4C, facilitating a more complete transition of silicon into nickel silicide (*NiSi*). The developed coatings possess a unique combination of high corrosion resistance, wear resistance, and adhesive strength. The obtained results recommend this technology for creating protective coatings for critical components in the oil and gas industry, shipbuilding, and energy sectors. Future research prospects include optimizing powder compositions and spraying parameters for various operational conditions, including elevated temperatures and combined loads.

For citation: Sirota V.V., Prokhorenkov D.S., Churikov A.S., Podgorny D.S., Alfimova N.I., Konnov A.V. Corrosion properties of coatings produced from self-fluxing powders by the detonation spraying method. *Obrabotka metallov (tekhnologiya, oborudovanie, instrumenty) = Metal Working and Material Science*, 2025, vol. 27, no. 3, pp. 151–165. DOI: 10.17212/1994-6309-2025-27.3-151-165. (In Russian).

*** Corresponding author**
Sirota Vyacheslav V., Ph.D. (Physics and Mathematics)
Belgorod State Technological University named after V.G. Shukhov,
46 Kostyukova st.,
308012, Belgorod, Russian Federation
Tel.: +7 904 539-14-08, **e-mail:** zmas36@mail.ru

Introduction

Modern wear-resistant coatings made of self-fluxing nickel-based alloys are widely used in industry [1]. However, when operating in aggressive environments, such as seawater or chemically active solutions, these coatings are subjected not only to mechanical stress but also to corrosive degradation. In this case, the corrosion rate can significantly affect their wear resistance and durability, leading to premature failure of components and substantial economic losses [2–4].

The relevance of this work lies in the need for a comprehensive study of the corrosion behavior of wear-resistant coatings, since their traditional evaluation is mainly limited to mechanical characteristics, such as hardness and abrasion resistance [5–8]. However, even high-strength coatings, for example, those based on tungsten or boron carbides, can lose their operational properties due to corrosion processes developing at particle boundaries or pores [9–12]. It is particularly important to investigate corrosion kinetics, as it determines not only the service life of the coating but also its interaction with the substrate, ultimately affecting the overall performance of the system [13–15].

In this study, the detonation spraying method was used to apply the coatings, which offers several significant advantages over alternative technologies. The key advantages of the detonation spraying method include: high particle velocity (up to 2,500 m/s), ensuring better coating adhesion to the substrate and reducing porosity [16], lower heating of the sprayed material, minimizing the risk of undesirable phase transformations and oxidation [17], and the ability to precisely control process parameters, including the gas mixture composition and explosion energy, allowing for optimization of the coating structure and properties [18].

The practical significance of this work lies in the potential application of the obtained results in the development of new wear- and corrosion-resistant coatings for equipment in the oil and gas industry, shipbuilding, and energy sectors operating under extreme conditions. The scientific novelty of the study consists in establishing quantitative relationships between the boron carbide content, detonation spraying parameters, and the corrosion resistance of nickel-chromium-boron-silicon coatings, which has not been previously addressed in the literature to such an extent.

The objective of this work was to evaluate the corrosion rate of wear-resistant coatings based on the self-fluxing alloy PR-NKh17SR4 and its modified counterpart with the addition of boron carbide.

The specific aims of this study were to:

– mechanically blend the self-fluxing powder *NiCrBSi* alloy (*PR-NKh17SR4*) with 10 % boron carbide (B_4C) and assess the uniformity of particle distribution;

– compare the granulometric composition and bulk density of the initial powders and the resulting mixture;

– study the microstructure of the coatings using scanning electron microscopy (*SEM*) and X-ray diffraction (*XRD*) analysis;

– perform electrochemical tests (potentiostatic measurements, impedance spectroscopy) in a 3.5 % *NaCl* solution,

– compare the corrosion behavior of *NiCrBSi* alloy (*PR-NKh17SR4*), *NiCrBSi* (*PR-NKh17SR4*)+10 wt. % B_4C coatings, and a commercial counterpart *NiCr/WC* alloy (*VSNGN-85*).

Methods

For the research, plates made of structural steel grade *0.4 C-Mn (40G)* (40×40×5 mm) were used as substrates. The chemical composition of the steel complies with the requirements of *GOST 1050-2013*. Spectral analysis performed on an optical emission spectrometer "*ISKROLINE 100*" (Russia) confirmed that the steel met the declared grade. The content of the main alloying elements was as follows: 0.40 % carbon, 0.25 % silicon, and 0.78 % manganese, with the total content of sulfur and phosphorus not exceeding 0.03 % each.

Substrate surface preparation involved thorough sandblasting with quartz sand (grain size 1.0±0.2 mm) at a compressed air pressure of 0.6 MPa.

For coating deposition, a multi-chamber cumulative detonation spraying setup (*MKDU*, BSTU named after V.G. Shukhov, Russia) was employed. A distinctive feature of this setup is its dual-chamber system with a focusing lens, enabling particle velocities of up to 2,500 m/s. The system is equipped with a precision gas mixture supply unit and an automated process parameter control system. The gas mixture composition (propane-butane/oxygen/air) was set at a ratio of 13/57/30 vol. %. The process parameters were optimized based on the authors' previous research [19–20].

Three types of powders were used as feedstock materials. The base material was the self-fluxing powder *NiCrBSi* alloy (*PR-NKh17SR4*) produced by *POLEMA JSC* (Russia). To prepare a composite mixture based on this self-fluxing powder, boron carbide grade *F1200* manufactured by *Promkhim LLC* (Russia) was used. The addition of 10 wt. % boron carbide was performed by mechanical mixing in a *Pulverisette 6* planetary mono-mill (*Fritsch*, Germany) at a rotation speed of 200 rpm for 120 minutes. The uniform distribution of boron carbide particles in the *NiCrBSi* alloy (*PR-NKh17SR4*) powder was visually confirmed by backscattered electron imaging (Fig. 1, *d*).

As a reference material, commercial powder *NiCr/WC* alloy (*VSNGN-85*) produced by *Technicord LLC* (Russia) was employed. This material was selected as a typical representative of wear-resistant coatings widely used in industry. The elemental composition of the initial powders was analyzed using energy-dispersive spectroscopy, particle morphology was determined by electron microscopy imaging, and apparent density was measured using a graduated cylinder. The characterization results of the initial powders are presented in Table 1.

Fig. 1 shows the morphology of the initial powders and prepared mixture.

The samples were prepared for microstructure and corrosion properties investigation using a precision cutting machine *IsoMet 5000* (*Buehler*, Germany) and a grinding-polishing machine *MetaServ 250* (*Buehler*, Germany). The final polishing was performed with a 3 μm *Carat* diamond polishing disc (*Labortek*, Russia). Porosity evaluation was conducted on coating cross-sections using the *SIAMS 800* hardware-software complex analyzer. The thickness of the deposited coatings was controlled with an ultrasonic thickness

Table 1

Characteristics of the initial powders

Material	Chemical composition, wt.%							Particle morphology	Apparent density, g/cm^3
	C	*Cr*	*Si*	*B*	*Fe*	*W*	*Ni*		
NiCrBSi alloy (*PR-NKh17SR4*)	1.0	17.1	4.1	3.6	4.8	–	bal.	Spherical	4.1±0.2
NiCrBSi (*PR-NKh17SR4*)+ 10 wt. % B_4C	3.1	15.0	3.5	11.1	4.3	–	bal.	Mixed spherical/angular	3.9±0.2
NiCr/WC alloy (*VSNGN-85*)	5.3	2.5	0.6	0.55	0.4	79.8	bal.	Agglomerated	7.0±0.2

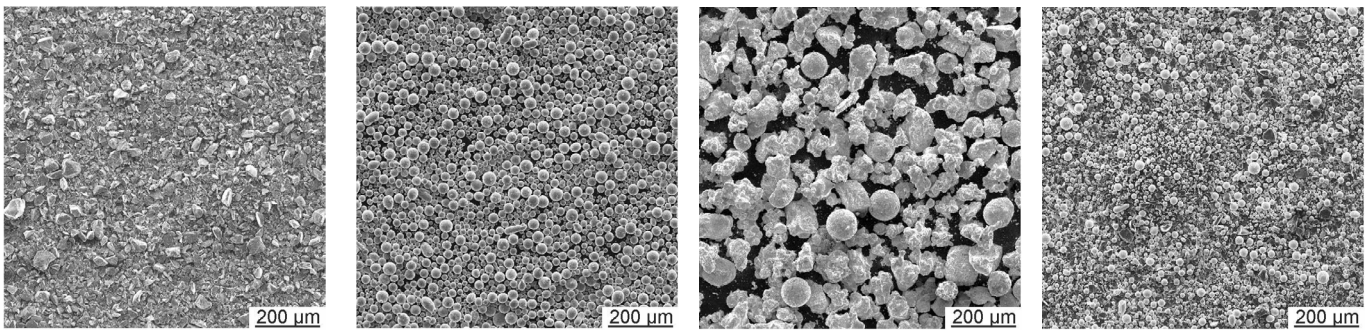

a *b* *c* *d*

Fig. 1. Micrographs of the initial powders and mixture. (*a*), (*b*), (*c*) *SE* images of B_4C, *NiCrBSi* (*PR-NKh17SR4*), and *NiCr/WC* (*VSNGN-85*) powders, respectively. (*d*) *BSE* image of the *NiCrBSi* (*PR-NKh17SR4*)+10 wt. % B_4C mixture

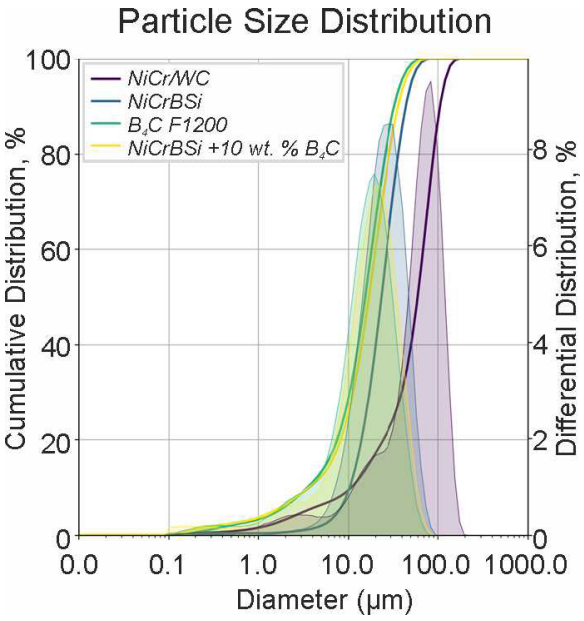

Fig. 2. Particle size distribution of the initial powders and mixture

gauge *45MG* (*Olympus*, Japan). The particle size distribution of the initial powders and mixture was determined using an *Analysette 22 NanoTec Plus* powder granulometry analyzer (*Fritsch*, Germany), as shown in Fig. 2.

The investigation of the obtained coatings was performed using a comprehensive set of modern analytical methods to thoroughly evaluate their structural and functional properties. Microstructural studies were conducted using a *Mira 3* scanning electron microscope (*Tescan*, Czech Republic) equipped with an *X-Max 50* energy-dispersive spectroscopy system and *AZtec* software (*Oxford* Instruments, UK). Secondary electron (*SE*) and backscattered electron (*BSE*) imaging, along with elemental composition analysis, were performed at an accelerating voltage of 15 kV and a working distance of 15 mm. The *EDS* data were processed using specialized *AZtec* software.

Porosity evaluation was carried out by analyzing *SEM* images of coating cross-sections with a 1,000 **μ**m field of view using *ImageJ* software.

The phase composition of the coatings was examined by X-ray diffraction analysis using an *ARL X'TRA* diffractometer with *Cu-K***α** radiation (**λ** = 1.5418 Å). Measurements were performed in **θ-2θ** scanning mode within the angular range of 10–90° with a step size of 0.02° and an exposure time of 1 s per point. Phase identification was conducted using the *PDF-2* database from the International Centre for Diffraction Data (*ICDD*).

Corrosion testing was performed using a three-electrode electrochemical cell with a *SmartStat PS-10-4* potentiostat-galvanostat. A 3.5 % sodium chloride solution (pH = 6.8±0.2), prepared from analytically pure ("chemically pure") grade reagent and distilled water, served as the working electrolyte. The reference electrode was a silver/silver chloride (*Ag*/*AgCl*) electrode, and the counter electrode was made of graphite.

The electrochemical testing protocol consisted of several sequential stages. Initially, the open circuit potential (*OCP*) was monitored for 60 minutes until it reached a steady-state condition (±10 mV/10 min). This was followed by electrochemical impedance spectroscopy (*EIS*) measurements across a frequency range of 50 kHz to 10 mHz with an *AC* signal amplitude of 10 mV. The obtained *Nyquist* spectra were fitted using equivalent electrical circuits with the "*impedance.py*" script [21]. Subsequently, potentiodynamic polarization curves were recorded at a scan rate of 1 mV/s, covering a potential range from −300 mV versus *OCP* to +1.2 V versus *Ag*/*AgCl*, or until reaching a current density of 10 mA/cm^2. Special attention was paid to analyzing the *Tafel* regions of both anodic and cathodic branches to determine kinetic parameters of the corrosion process. For each sample, a minimum of three replicate tests were conducted, followed by statistical analysis of the results.

Post-corrosion characterization included surface examination using scanning electron microscopy. The depth of corrosion penetration was evaluated using a confocal laser microscope with a vertical resolution of 10 nm.

Mechanical tests involved *Vickers* microhardness measurement criteria on a *NEXUS 4504-IMP* hardness tester (*INNOVATEST*, Netherlands) at 1 kg and a holding time of 15 s. For each sample, at least 10 measurements were made with subsequent exclusion of gross errors using the *Student* criterion.

Results and Discussion

A comprehensive study of the coating microstructure revealed significant differences between the studied compositions. The coating based on the self-fluxing powder *NiCrBSi* (*PR-NKh17SR4*) demonstrated

a characteristic layered structure with clearly defined boundaries between individual sprayed particles (Fig. 3, *a*). The average size of the structural elements was 10–30 **μ**m, which corresponds to the granulometry of the original powder. The porosity determined by quantitative image analysis did not exceed 0.7±0.1 %, with most of the pores located at the interparticle boundaries.

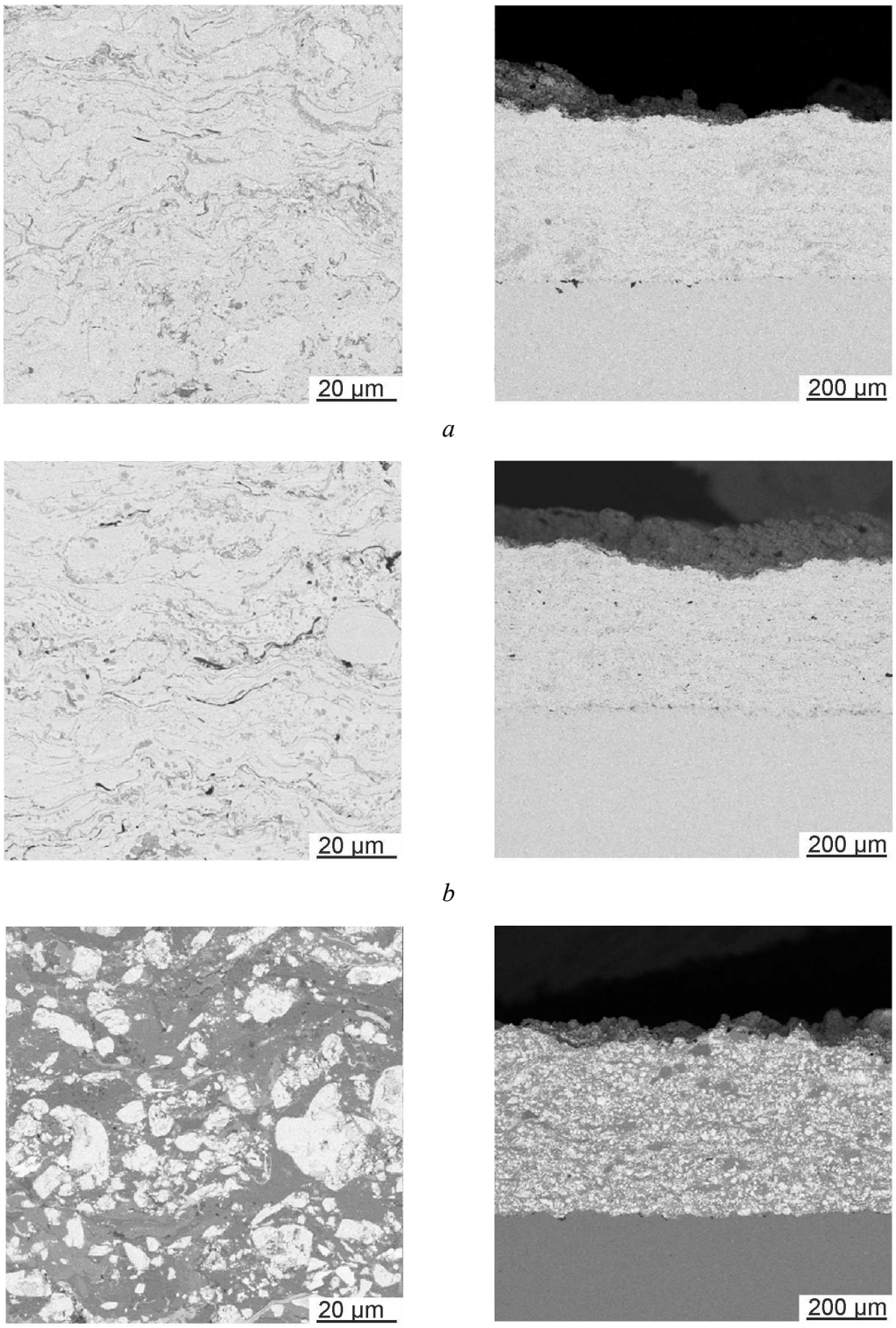

Fig. 3. SEM images of the cross-sectional microstructure of the coatings:
a – NiCrBSi (*PR-NKh17SR4*); *b – NiCrBSi* (*PR-NKh17SR4*)+10 wt.% B_4C; *c – NiCr/WC* (*VSNGN-85*)

The introduction of 10 % boron carbide resulted in a significant change in the microstructure (Fig. 3, *b*). While maintaining the average size of the structural elements and porosity at the same level (Table 2), a qualitative change in the boundaries between individual sprayed particles was observed.

Table 2

Structural characteristics of the studied coatings

Parameter	*NiCrBSi* (*PR-NKh17SR4*)	*NiCrBSi* (*PR-NKh17SR4*)+10 % B_4C	*NiCr/WC* (VSNGN-85)
Average thickness, μm	410±15	390±40	430±30
Porosity, %	0.7±0.1	0.6±0.1	0.9±0.3
Hardness HV_1	520±30	680±40	1,250±120

EDS analysis showed saturation of grain boundaries with boron and the total boron content close to the added one (see Fig. 4). At the same time, the content of boron carbide particles was significantly lower than in the initial mixture. This indirectly indicates partial decomposition of boron carbide and active interaction of boron with other components of the coating in the process. X-ray phase analysis also showed the presence of an amorphous peak and broadening of the base of the nickel peak, which confirms the formation of solid solutions in greater quantities compared to the *NiCrBSi* (*PR-NKh17SR4*) coating (see Fig. 5). For data processing and quantitative phase analysis, the *Rietveld* method implemented in the *Match3* software was used, which allows for taking into account the overlap of peaks and the influence of microstructural factors.

The *NiCr/WC* (*VSNGN-85*) coating has a characteristic "island" structure with clearly defined tungsten carbide particles in a nickel matrix (see Fig. 3, *c*). X-ray phase analysis also showed sharp peaks of tungsten carbide against the background of diffuse peaks corresponding to nickel-based solid solutions. The results of electrochemical studies showed a significant effect of the coating composition on their corrosion behavior in a 3.5 % *NaCl* solution. Potentiometric measurements revealed significant differences in the corrosion potential values (Fig. 7, *a*). The most noble potential (−250±30 mV) was recorded for the *NiCrBSi* (*PR-NKh17SR4*)+10 % B_4C coating, which indicates its increased thermodynamic stability.

Analysis of the polarization curves (Fig. 6) revealed that the boron carbide-modified coating exhibited the lowest corrosion current density (0.8±0.02 μA/cm^2), which was an order of magnitude lower than that of the base composition (6.5±0.2 μA/cm^2). Electrochemical impedance spectroscopy confirmed the formation of a dense protective film on the modified coating surface, as evidenced by the high polarization resistance values (215±25 kOhm·cm² and low constant phase element parameters (45±5 μF·cm^{-2}·s^{-1}).

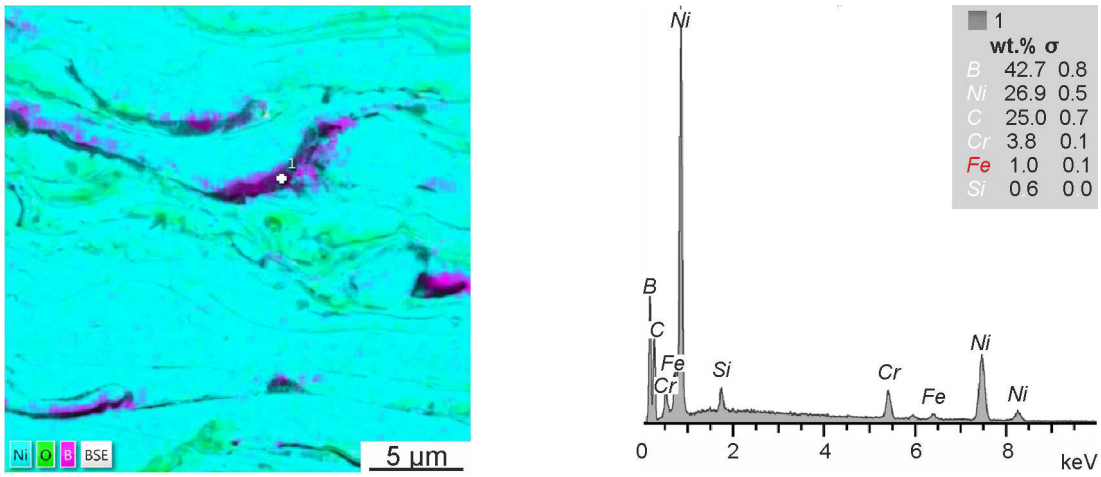

Fig. 4. EDS mapping of the cross-section of *NiCrBSi* (*PR-NKh17SR4*)+10 wt.% B_4C

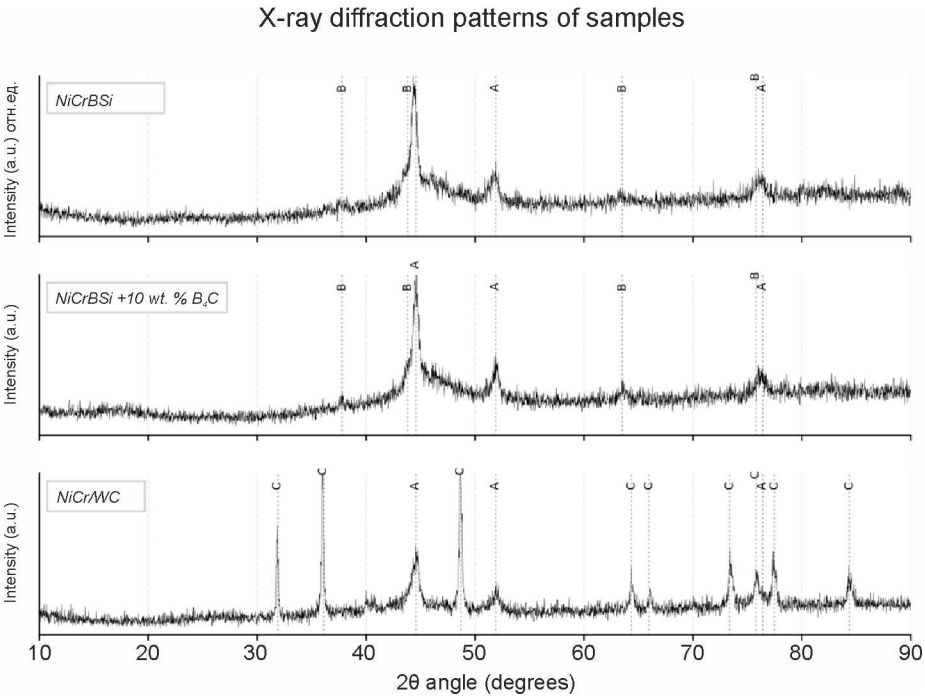

Fig. 5. XRD patterns of the studied coatings:
A – Fm-3m (***a*** = 0.350 ± 0.003 nm) Solid solutions of interstitial and substitutional types based on nickel; ***B*** – Fm-3m (***a*** = 0.414 ± 0.003 nm) Intermetallic compounds; ***C*** – P-6m2 (***a*** = 0.291 nm, ***c*** = 0.284 nm) – Tungsten carbide (*WC*)

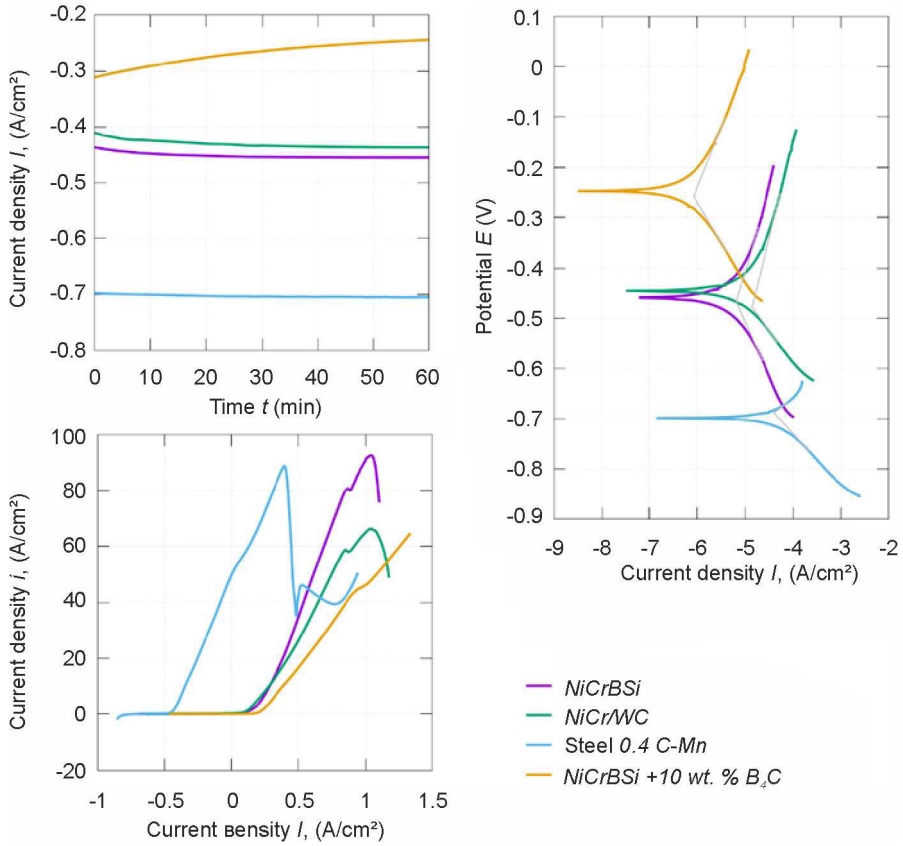

Fig. 6. Kinetics of the open circuit potential (*OCP*) establishment (left top); linear polarization curves (bottom left); and *Tafel* plots (right) in an aqueous solution containing 3.5% *NaCl*. Potential data are given relative to a silver/silver chloride (Ag/AgCl) electrode

The *Tafel* slopes for both anodic and cathodic reactions were determined from polarization curves plotted in semi-logarithmic coordinates (see Fig. 6), enabling calculation of corrosion current densities and potentials (Table 3). The results demonstrated that the boron carbide-modified coating exhibited the lowest corrosion current density (0.8 μA/cm^2), which was one order of magnitude lower than both the base *NiCrBSi* (*PR-NKh17SR4*) composition (6.5 μA/cm^2) and the *NiCr*/*WC* (*VSNGN-85*) coating (13.9 μA/cm^2).

Table 3

Corrosion behavior parameters in 3.5 % *NaCl*

Parameter	Steel *0.4 C-Mn*	*NiCrBSi* (*PR-NKh-17SR4*)	*NiCrBSi* (*PR-NKh-17SR4*)+10 % B_4C	*NiCr*/*WC* (*VSNGN-85*)
E_{corr} (vs. *SCE*) (mV)	−690±15	-470±10	−260±10	−480±12
i_{corr} (μA/cm²)	40.2±1.5	6.5±0.2	0.8±0.02	13.9±0.4
R_{ct} (kΩ·cm²)	0.4±0.1	6.6±0.8	66.4±5.2	3.1±1.0
QCPE (μF·cm^{-2}·s^{-1})	0.3	600	240	1100
n	1	0.63	0.66	0.6

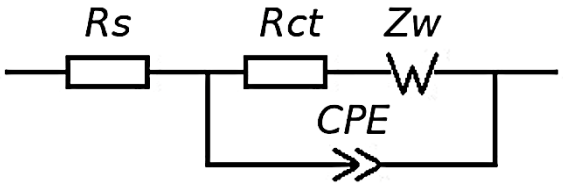

Fig. 7. Randles-Ershler equivalent circuit

Electrochemical impedance spectroscopy studies in 3.5 % *NaCl* aqueous solution revealed that the impedance data for all investigated coatings fitted well with the *Randles-Ershler* equivalent circuit model (Fig. 7). In this circuit, the constant phase element (*CPE*) describes the double layer capacitance, R_{ct} represents the charge transfer resistance, and *ZW* corresponds to *Warburg* impedance associated with diffusion processes. The typical *Nyquist* plot featured a semicircular segment that rapidly transitioned into a sloping straight line (diffusion impedance) in the high-frequency region. However, the *NiCr*/*WC* (*VSNGN-85*) coating exhibited several inflection points, attributed to the presence of large heterogeneous phases (tungsten carbide and binder).

The electrochemical impedance spectroscopy data of the coatings and the substrate with superimposed approximation lines using the *Randles-Erschler* equivalent circuit are presented in Fig. 8 as *Nyquist* plots. The approximation parameters (see Table 3) confirmed the formation of a dense protective film on the surface of the *NiCrBSi* (*PR-NKh17SR4*)+10 wt.% B_4C coating, as evidenced by high values of polarization resistance and low values of the phase element constant. The low degree index of the studied coatings (0.6–0.7) indicates the heterogeneity and porosity of the coatings, which is consistent with the microstructure (see Fig. 3). At the same time, for the *NiCrBSi* (*PR-NKh17SR4*)+10 wt.% B_4C coating, this parameter is higher for the others, that is, it indicates higher homogeneity and lower porosity.

After corrosion tests, the surface of the coatings was examined using electron microscopy methods (see Fig. 9).

On the *NiCrBSi* (*PR-NKh17SR4*)+10 wt.% B_4C coating, shallow, predominantly surface corrosion was observed, while on the reference *NiCr*/*WC* (*VSNGN-85*) coating, numerous deep corrosion lesions of the metal bond were noted along the boundaries of tungsten carbide particles.

Conclusion

1. The conducted study allowed us to comprehensively evaluate the corrosion properties of self-fluxing powder coatings obtained by detonation spraying. The results showed that the introduction of 10 % boron

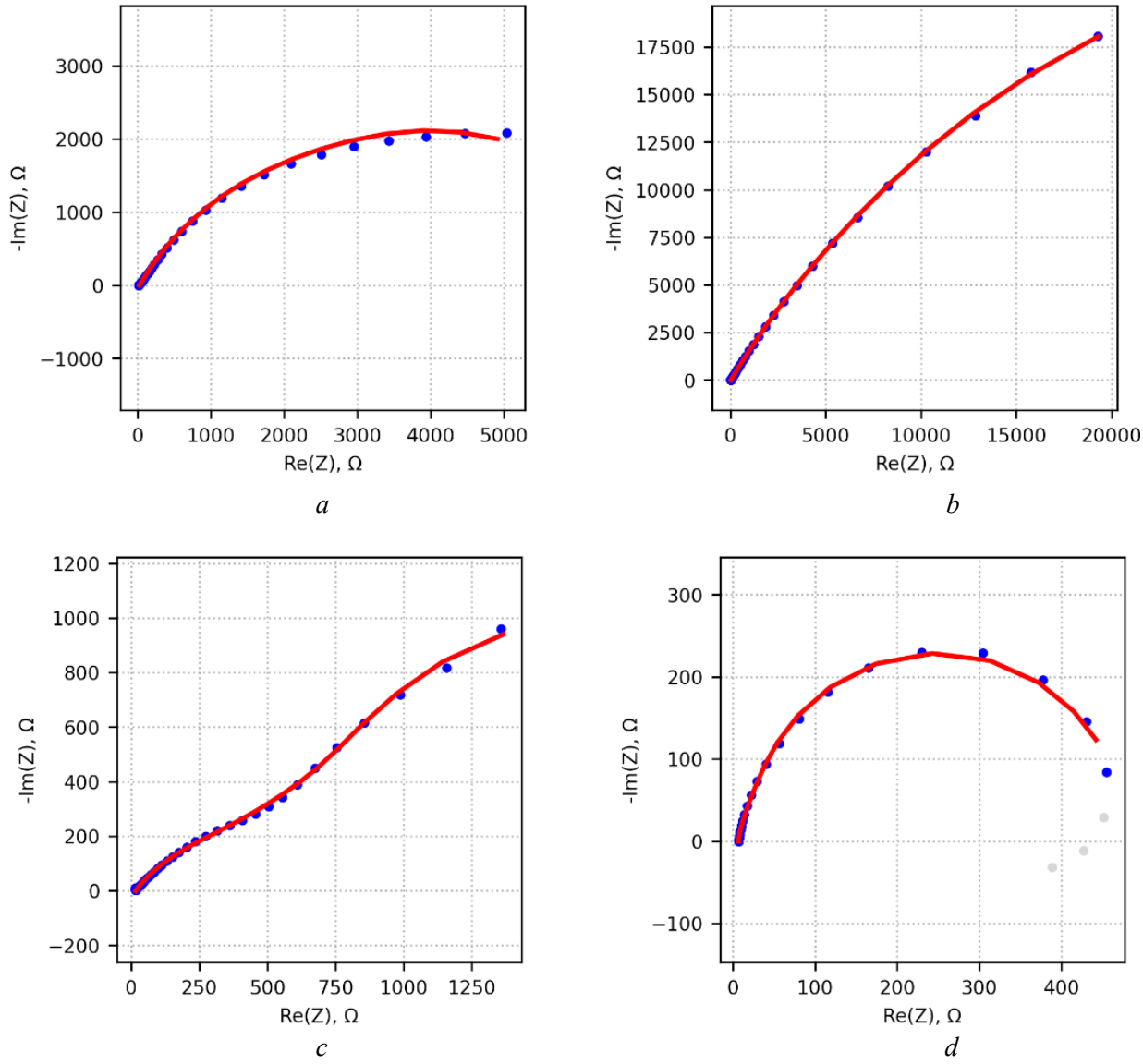

Fig. 8. Nyquist plots of coatings in an aqueous solution containing 3.5% *NaCl* near the stationary potential in the frequency range from 50 kHz to 10 MHz:
a – NiCrBSi PR-NKh17SR4); *b – NiCrBSi* (*PR-NKh17SR4*)+10 wt.% B_4C; *c – NiCr/WC* (*VSNGN-85*); *d – 0.4% C-Mn*

carbide into the self-fluxing alloy *NiCrBSi* (*PR-NKh17SR4*) significantly improves the corrosion resistance of the coating.

2. The modified coating demonstrates the most noble corrosion potential (−260±10 mV) and the minimum corrosion current (0.8±0.02 **μ**A/cm^2), which indicates its high thermodynamic and kinetic stability in an aggressive environment. These indicators significantly exceed the characteristics of both the base alloy *NiCrBSi* (*PR-NKh17SR4*) and the commercial coating *NiCr/WC* (*VSNGN-85*).

3. Microstructural analysis revealed that boron carbide promotes the formation of a dense multilayer protective system, including an external passivation layer based on chromium and boron oxides, a main matrix with dispersed NiB_2 particles, and an increase in the volume of the *NiSi* phase. Such a structure not only reduces the porosity of the coating, but also provides effective protection against the development of general and crevice corrosion.

4. Impedance spectroscopy confirmed the formation of a dense protective film, as evidenced by high values of polarization resistance (215±25 kOhm cm^2) and low values of the phase element constant.

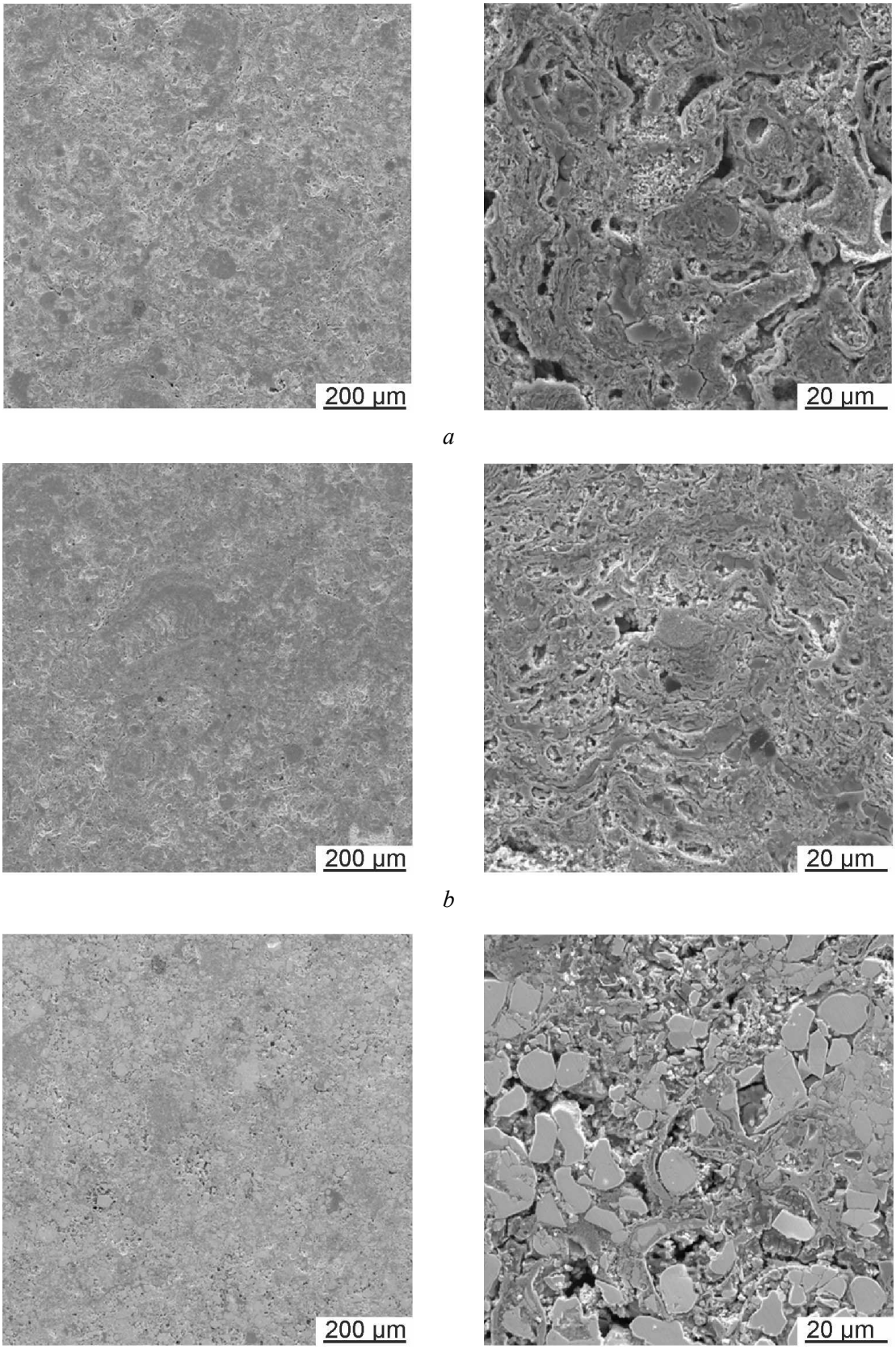

Fig. 9. SEM images of the surface microstructure after corrosion tests:
a – NiCrBSi (*PR-NKh17SR4*); *b – NiCrBSi* (*PR-NKh17SR4*)+10 wt.% B_4C
and *c – NiCr/WC* (*VSNGN-85*)

References

1. Simunovic K., Saric T., Simunovic G. Different approaches to the investigation and testing of the Ni-based self-fluxing alloy coatings – A review. Part 1: General facts, wear and corrosion investigations. *Tribology Transactions*, 2014, vol. 57 (6), pp. 955–979.

2. Koch G.H., Brongers M.P.H., Thompson N.G., Virmani Y.P., Payer J.H. Cost of corrosion in the United States. *Handbook of environmental degradation of materials*. William Andrew Publishing, 2005, pp. 3–24. DOI: 10.1016/B978-081551500-5.50003-3.

3. Thompson N.G., Yunovich M., Dunmire D. Cost of corrosion and corrosion maintenance strategies. *Corrosion Reviews*, 2007, vol. 25 (3–4), pp. 247–262. DOI: 10.1515/CORRREV.2007.25.3-4.247.

4. Baorong H.O.U., Dongzhu L.U. Corrosion cost and preventive strategies in China. *Bulletin of Chinese Academy of Sciences*, 2018, vol. 33 (6), pp. 601–609. DOI: 10.16418/j.issn.1000-3045.2018.06.008. (In Chinese).

5. Mariani F.E., Rêgo G.C., Neto A.L., Totten G.E., Casteletti L.C. Wear behavior of a borided nickel-based self-fluxing thermal spray coating. *Materials Performance and Characterization*, 2016, vol. 5 (4). DOI: 10.1520/MPC20150064.

6. Vidaković I., Šimunović K., Heffer G., Špada V. Microstructural analysis of flame-sprayed and PTA-deposited nickel-based self-fluxing alloy coatings. *Welding in the World*, 2024, vol. 68 (11), pp. 2819–2836. DOI: 10.1007/s40194-024-01814-5.

7. Kretinin V.I., Teppoev A.V., Sokolova V.A., Polyanskaya O.A., Alekseeva S.V. Justification of strengthening of working bodies of forestry machines with self-fluxing alloys during gas-flame spraying. *IOP Conference Series: Earth and Environmental Science*, 2021, vol. 876 (1), p. 012045. DOI: 10.1088/1755-1315/876/1/012045.

8. Dong X.Y., Luo X.T., Zhang S.L., Li C.J. A novel strategy for depositing dense self-fluxing alloy coatings with sufficiently bonded splats by one-step atmospheric plasma spraying. *Journal of Thermal Spray Technology*, 2020, vol. 29, pp. 173–184. DOI: 10.1007/s11666-019-00943-4.

9. Liu C.W., Qin E.W., Chen G.X., Wei S.C., Zou Y., Ye L., Wu S.H. Effect of flame remelting on the microstructure, wear and corrosion resistance of HVOF sprayed NiCrBSi coatings. *Advanced Materials Research*, 2024, vol. 1179, pp. 157–168. DOI: 10.4028/p-v2xcOL.

10. Shuecamlue S., Taman A., Khamnantha P., Banjongprasert C. Influences of flame remelting and WC-Co addition on microstructure, mechanical properties and corrosion behavior of NiCrBSi coatings manufactured via HVOF process. *Surfaces and Interfaces*, 2024, vol. 48, p. 104135. DOI: 10.1016/j.surfin.2024.104135.

11. Shabanlo M., Amini Najafabadi R., Meysami A. Evaluation and comparison the effect of heat treatment on mechanical properties of NiCrBSi thermally sprayed coatings. *Anti-Corrosion Methods and Materials*, 2018, vol. 65 (1), pp. 34–37. DOI: 10.1108/ACMM-02-2017-1756.

12. Xuan H.N., Chen L., Li N., Wang H., Zhao C., Bobrov M., Lu S., Zhang L. Temperature profile, microstructural evolution, and wear resistance of plasma-sprayed NiCrBSi coatings under different powers in a vertical remelting way. *Materials Chemistry and Physics*, 2022, vol. 292, p. 126773. DOI: 10.1016/j.matchemphys.2022.126773.

13. Fayomi O.S.I., Akande I.G., Odigie S. Economic impact of corrosion in oil sectors and prevention: an overview. *Journal of Physics: Conference Series*, 2019, vol. 1378 (2), p. 022037. DOI: 10.1088/1742-6596/1378/2/022037.

14. Kania H. Corrosion and anticorrosion of alloys/metals: the important global issue. *Coatings*, 2023, vol. 13 (2), p. 216. DOI: 10.3390/coatings13020216.

15. Shekari E., Khan F., Ahmed S. Economic risk analysis of pitting corrosion in process facilities. *International Journal of Pressure Vessels and Piping*, 2017, vol. 157, pp. 51–62. DOI: 10.1016/j.ijpvp.2017.08.005.

16. Zlobin S.B., Ulianitsky V.Yu., Shtertser A.A., Smurov I. High-velocity collision of hot particles with solid substrate, under detonation spraying: detonation splats. *Thermal Spray: Expanding Thermal Spray Performance to New Markets and Applications*. ASM, 2009, pp. 714–717. DOI: 10.31399/asm.cp.itsc2009p0714.

17. Tucker R.C. Jr. Structure property relationships in deposits produced by plasma spray and detonation gun techniques. *Journal of Vacuum Science and Technology*, 1974, vol. 11 (4), pp. 725–734. DOI: 10.1116/1.1312743.

18. Sundararajan G., Sen D., Sivakumar G. The tribological behaviour of detonation sprayed coatings: the importance of coating process parameters. *Wear*, 2005, vol. 258 (1–4), pp. 377–391. DOI: 10.1016/j.wear.2004.03.022.

19. Sirota V.V., Zaitsev S.V., Prokhorenkov D.S., Limarenko M.V., Skiba A.A., Churikov A.S., Dan'shin A.L. Detonation application of a hard composite coating to cutters for centrifugal beet shredders. *Russian Engineering Research*, 2023, vol. 43 (9), pp. 1142–1145. DOI: 10.3103/s1068798x23090216.

20. Sirota V.V., Zaitsev S.V., Limarenko M.V., Churikov A.S., Podgornyi D.S. The effect of the introduction of B4C on the adhesive and cohesive properties of self-fluxing coatings. *Construction Materials and Products*, 2024, vol. 7 (6). DOI: 10.58224/2618-7183-2024-7-6-5.

21. Murbach M.D., Gerwe B., Dawson-Elli N., Tsui L. impedance.py: A Python package for electrochemical impedance analysis. *Journal of Open Source Software*, 2020, vol. 5 (52), p. 2349. DOI: 10.21105/joss.02349.

Conflicts of Interest

The authors declare no conflict of interest.